

Modeling of Respiratory Lung Motion as a Contact Problem of Elasticity Theory

René Werner*, Jan Ehrhardt, and Heinz Handels

Department of Medical Informatics, University Medical Center Hamburg-Eppendorf, Germany

*Corresponding author: Martinistr. 52, D-20246 Hamburg, Germany; r.werner@uke.uni-hamburg.de

Abstract: Breathing motion is a major problem in radiotherapy of lung tumors. The development of techniques to adequately account for respiratory motion requires detailed knowledge about breathing dynamics. Thus, computer aided modeling of respiratory motion gains in importance. In this paper we present an approach to model respiratory lung model. Main aspects of the process of lung ventilation are formulated as a contact problem of elasticity theory; the corresponding boundary value problem is solved by COMSOL Multiphysics. The influence of biomechanical parameters on the modeling process is analyzed. Modeling accuracy is evaluated using 4D(=3D+t) CT data of lung tumor patients. Differences of inner lung landmark motion amplitudes observed within the CT data and motion amplitudes predicted model based are in the order of 3 mm; the impact of the elastic constants is fairly small. Results show that FE-modeling is an adequate strategy to model aspects of the physiology of breathing.

Keywords: biomechanical modeling, respiratory lung motion, 4D CT, radiotherapy

1 Introduction

Respiratory motion is main problem in radiation therapy (RT) of lung tumors. To achieve high local tumor control and low normal tissue complication probabilities the dose applied should be focused on tumor tissue while avoiding organs at risk (normal tissues influencing treatment planning and/or prescribed dose [2]) like the lungs. This becomes challenging in case of lung tumors as organs and tumors move due to respiration. In recent years methods have been developed to explicitly account for respiratory motion in RT such as real-time tumor-tracking [4, 9] or gated radiation therapy

[7, 3]. However, the clinical use of these techniques is still controversial; various authors emphasize that further detailed analysis of respiratory dynamics is needed [5].

A main issue within this field of research is the process of lung motion modeling. On the one hand it helps to get a deeper understanding of respiratory motion itself. Resulting simulations, on the other hand, can be applied to problems of direct clinical importance, e. g. to investigate the impact of respiratory motion on the dose distribution in organs at risk and target volumes. We propose to use COMSOL Multiphysics to model respiratory lung motion as a contact problem of elasticity theory taking the physiology of breathing as starting point of modeling. Our study consists of two parts: First, we analyze the impact of biomechanical parameters on the modeling process. This is accomplished by means of a mathematical lung phantom. The modeling approach proposed allows for patient specific modeling. Thus, as the second part of the study, we use 4D(=3D+t) CT data of lung tumor patients to generate patient specific models in order to evaluate the modeling accuracy.

2 Methods and Materials

2.1 Modeling approach and governing equations

Macroscopic lung motion is mainly driven by the process of lung ventilation. The lungs are not moving actively. They are located in the pleural cavity built up by the parietal pleura (adherent to the internal surface of the thoracic cavity and the diaphragm) and the visceral pleura (adherent to the lung surface). Both pleurae are joined together at the root of the lung. The space enclosed is filled with a liquid and it is subjected to a negative pressure called intrapleural pressure. Contraction of breathing muscles (di-

aphragm, outer intercostals) causes the thoracic cavity to expand. This in turn changes the intrapleural pressure which acts as a surface force upon the lung surface. Thus, lung expands. During lung expansion the visceral pleura is, due to the liquid within the pleural cavity, sliding down the internal surface of the thoracic cavity frictionlessly.

Based on a modeling idea by Zhang et al. [14] we model the process of lung ventilation as a contact problem of elasticity theory. A uniform negative pressure p_{intrapl} representing the intrapleural pressure is applied to the surface Γ_1 of an initial lung geometry Ω_1 (except for the area Γ_2 of the root of the lung which is assumed to be fixed). The initial lung geometry represents the lung at the phase of end-expiration (EE). Intrapleural pressure magnitude is increased gradually starting with a zero pressure. This causes Ω_1 to expand. Expansion is limited by a geometry Ω_2 representing the shape of the lung at a final state of breathing (Ω_2 and corresponding surfaces Γ_3 and Γ_4 are considered to be fixed); in this study we choose the final state to be end-inspiration (EI). Principle and nomenclature are illustrated in Figure 1.

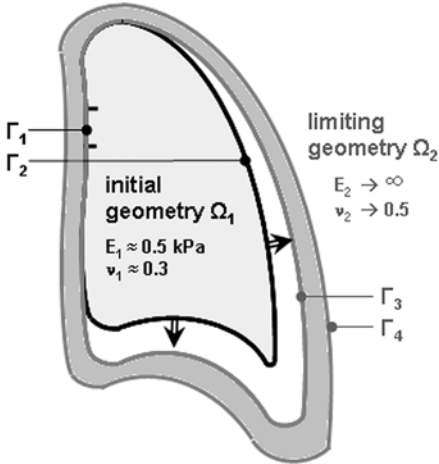


Figure 1: Illustration of the contact problem considered: Ω_1 represents a lung at end-expiration which expands due to a negative pressure applied to the lung surface. Lung expansion is limited by a second geometry Ω_2 representing the lung shape at end-inspiration.

We assume lung tissue to be isotropic, homogeneous, and linear elastic. This assumption is a simplistic one but it enables to model lung elasticity by means of general-

ized Hooke's law. Thus, the contact problem to be solved is given by:

Governing equations:

$$\begin{aligned} \nabla \sigma &= \mathbf{0} \quad \text{in } \tilde{\Omega} \\ \varepsilon &= \frac{1}{2} (\nabla \mathbf{u} + \nabla \mathbf{u}^T + \nabla \mathbf{u}^T \nabla \mathbf{u}) \quad \text{in } \Omega \\ \mathbf{S} &= \mathbf{C} \varepsilon \quad \text{in } \Omega \end{aligned}$$

whereas

$$\begin{aligned} \sigma &= (1/\det \mathbf{F}) \mathbf{F} \mathbf{S} \mathbf{F}^T \\ \mathbf{F} &= \nabla \mathbf{u} + \mathbf{I} \end{aligned}$$

Boundary conditions:

$$\begin{aligned} \mathbf{u} &= \mathbf{0} \quad \text{in } \Gamma_1 \cup \Gamma_3 \cup \Gamma_4 \\ \sigma \mathbf{n} &= (p_{\text{intrapl}} + p_{\text{contact}}) \mathbf{n} \quad \text{in } \tilde{\Gamma}_2 \end{aligned}$$

Contact conditions on $\tilde{\Gamma}_2$:

$$\begin{aligned} g &\leq 0 \\ p_{\text{contact}} &\leq 0 \\ p_{\text{contact}} \cdot g &= 0 \end{aligned}$$

where $\Omega = \Omega_1 \cup \Omega_2$ represents the domain in its undeformed state, $\tilde{\Omega}$ is the domain after deformation, \mathbf{u} states the displacement field which represents the estimate of the inner lung motion field between EE and EI, and $\mathbf{C} = \mathbf{C}(E, \nu)$ is the elasticity tensor depending on Young's modulus E and Poisson's ratio ν . The contact conditions are given by the Signorini conditions, i. e., in case of contact between Γ_2 and Γ_3 compressive contact forces $p_{\text{contact}} \mathbf{n}$ are introduced in order to prevent penetration (g : normal gap, distance between Γ_2 and Γ_3). Large deformations are considered to be possible (lung volume changes due to respiration are in the order of 20 % of the lung volume at EE); thus, we consider Green-Lagrange strain ε and 2nd Piola-Kirchhoff stress \mathbf{S} where \mathbf{S} and Cauchy stress σ are linked by the deformation gradient \mathbf{F} .

2.2 Implementation

The contact problem of elasticity theory is solved by means of the Augmented Lagrangian method provided by the Structural Mechanics Module of COMSOL Multiphysics. The modeling process aims at the state where the surface $\tilde{\Gamma}_2$ of the deformed initial geometry and the surface Γ_3 of the limiting geometry nearly match. In our study we define a volume ratio of 0.995 between $\tilde{\Omega}_1$ and Ω_2 as the success criterion, i. e., the intrapleural pressure is increased

until a volume ratio of 0.995 is reached. As element type we use tetrahedrons with linear with linear shape functions.

In previous literature there is no consensus on values of the elastic constants when modeling lung tissue to behave linear elastically [14, 12, 1]. In the first part our study we analyze the influence of different E and ν values on the modeling process (i. e., the intrapleural pressure needed to reach a volume ratio of 0.995) and resulting motion field estimates \mathbf{u} . Therefore we adapt a mathematical lung phantom given by Staniszevska [10] who proposes to represent the lung shapes as a modification of quarters of an ellipsoid. Lung shapes are defined by the build-in CAD tool of COMSOL Multiphysics. E and ν values are varied within the scope of literature values (E values between 0.25 and 1.0 kPa, ν ranges from 0.1 to 0.45).

To evaluate modeling accuracy we generate patient specific models. This second part of the study is based on 4D CT data of lung tumor patients. Given the CT data at EE and EI we segment the lungs and generate lung surface models by means of the Marching Cubes algorithm [6]. After smoothing the surface models by a Laplacian smoother the surface models are imported to COMSOL Multiphysics via STL files serving as geometry descriptions Ω_1 and Ω_2 . The elastic constants are chosen according to the results of the phantom study. Mod-

eling accuracy is evaluated by comparing simulated patient specific motion patterns of inner lung landmarks (prominent bifurcations of bronchial and vessel trees within the lungs) with corresponding motion patterns as observed in the 4D CT data.

3 Results

Increasing Young's modulus E and/or Poisson's ratio ν produces stiffer response to external forces. Thus, higher E and ν values require higher values of the intrapleural pressure to fulfill the volume ratio of 0.995 (i. e., to get the deformed initial and the limiting geometry in close contact). Besides, the influence of different E and ν values on the motion field estimate \mathbf{u} can be shown to be fairly small: Based on the mathematical lung phantom mean differences between corresponding displacement vectors are in the order of 0.2 mm (max. differences ≤ 1 mm). Results are based on FE meshes consisting of approx. 25 000 tetrahedrons; corresponding displacement vectors are obtained by voxelization of Ω_1 .

Based on the results of the phantom study the elastic constants are chosen to be $E=0.5$ kPa and $\nu=0.3$ when generating the patient specific models. In Figure 2 a patient specific lung shape at EE and the corresponding shape at simulated EI are shown.

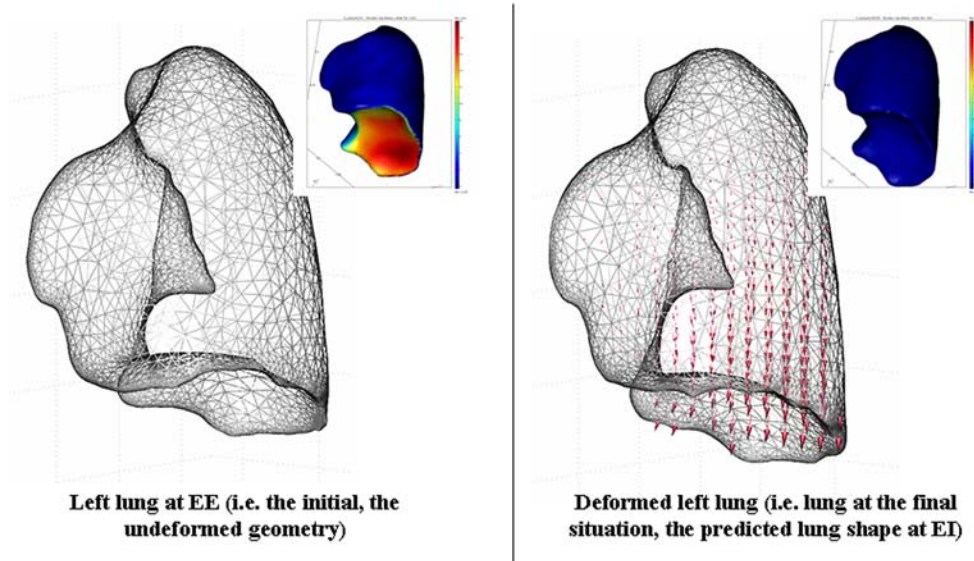


Figure 2: Surface mesh for a left lung at EE (left) and simulated EI (right). The arrows indicate the direction of motion. The small pictures in each right upper corner show the gap distance (red: distance up to 20 mm; blue: almost no distance). Figure taken from [13].

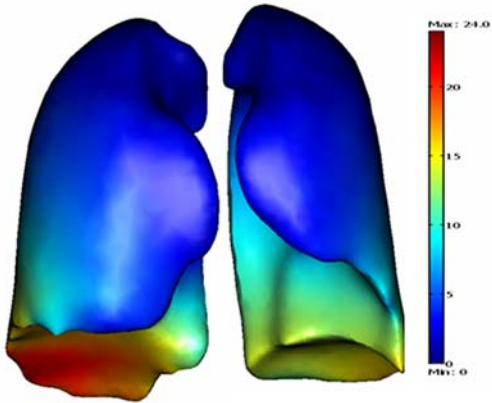


Figure 3: Color coded visualization of the distance of the surface points with respect to their initial positions as simulated model-based (in mm).

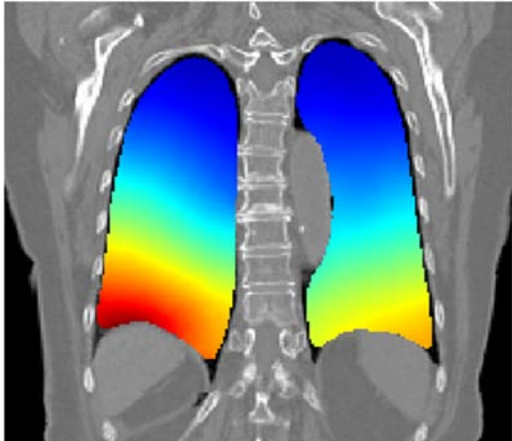


Figure 4: Visualization of inner lung displacement vector amplitudes as given by the FEM model, shown for a coronal view (same color bar as in Figure 3).

In Figure 3 and 4 corresponding motion field estimates between EE and EI are visualized. Discretized lung geometries of the patient specific models consist of between 60 000 and 170 000 tetrahedrons; solving times are between 15 and 70 min (two Intel Xeon dual-core processors, 16 GB RAM) where the increment in intrapleural pressure has been chosen to 5 N/m². Our results are based on a total of 12 lung tumor patients. To evaluate modeling accuracy we identified 20 landmarks in the middle of the lung, 15 landmarks near the lung borders (which are the information bearing structures of the modeling process), and 10 landmarks close to the lung tumor (if existent) for each lung. Mean landmark motion amplitude is 6.6±5.2 mm (max. landmark motion is >30 mm); intraobserver variability in landmark detection is 0.9±0.8 mm.

No systematic over- or underestimation of landmark motion prediction is apparent in lateral, anteroposterior, or craniocaudal direction. The registration residual (= difference of predicted landmark motion amplitude and the landmark motion amplitude as observed by manual landmark motion detection) is 3.3±2.1 mm. Only small differences in motion prediction quality appear for landmarks in the middle of the lung and landmarks close to lung border. This also holds for landmarks close to the tumor and else landmarks – except for the case of big lung tumors (see table 1). As a general tendency the modeling accuracy seems to decrease with increasing tumor size.

Landmarks	Registration residual in mm			
	no tumor	small tumor	midsize tumor	big tumor
in the middle of the lung	2.8 ± 1.5	2.9 ± 1.6	4.1 ± 2.6	4.2 ± 2.6
near the pleura	2.9 ± 1.8	3.3 ± 1.7	4.4 ± 2.2	4.2 ± 2.3
close to the tumor	—	3.0 ± 1.5	4.1 ± 2.2	6.3 ± 3.1
mean	2.8 ± 1.6	3.1 ± 1.6	4.2 ± 2.4	4.6 ± 2.7

Table 1: Registration residual values listed according to tumor size and landmark location (small tumor: tumor volume < 14 cm³; midsize tumor: tumor volume between 14 cm³ and 65 cm³; big tumor: tumor volume > 65 cm³; classification based on [8]).

4 Conclusions

Outcomes show that, on the one hand, the modeling approach allows estimating lung

motion in a reasonable way: Registration residuals obtained for the patient specific models are in the order of corresponding values published by other authors and other

modeling approaches (see e. g. [11]) when focusing on the lung models containing only a small lung tumor or without tumor. On the other hand, decreasing modeling accuracy with increasing tumor size indicates that assuming lung tissue to be linear elastic, homogeneous, and isotropic could be an oversimplifying assumption. Thus, the influence of tumorous tissue within the lung on elastic properties of the lung should be analyzed in more detail on both global and local scale. Corresponding results could be integrated into the modeling approach proposed.

References

- [1] A. Al-Mayah, J. Moseley, and K.K. Brock, *Contact surface and material nonlinearity modeling of human lungs.*, Phys Med Biol **53** (2008), no. 1, 305–317.
- [2] ICRU50, *Prescribing, recording, and reporting photon beam therapy*, ICRU report, no. 50, Bethesda, Md., International Commission on Radiation Units and Measurements, 1993.
- [3] S.B. Jiang, *Technical aspects of image-guided respiration-gated radiation therapy.*, Med Dosim **31** (2006), no. 2, 141–151.
- [4] P.J. Keall, S. Joshi, S.S. Vedam, J.V. Siebers, V.R. Kini, and R. Mohan, *Four-dimensional radiotherapy planning for dmhc-based respiratory motion tracking.*, Med Phys **32** (2005), no. 4, 942–951.
- [5] X.A. Li, P.J. Keall, and C.G. Orton, *Point/counterpoint. respiratory gating for radiation therapy is not ready for prime time.*, Med Phys **34** (2007), no. 3, 867–870.
- [6] W.E. Lorensen and H.E. Cline, *Marching cubes: A high resolution 3-d surface construction algorithm*, Comput Graph **21** (1987), 163–9.
- [7] G.S. Mageras and E. Yorke, *Deep inspiration breath hold and respiratory gating strategies for reducing organ motion in radiation treatment.*, Semin Radiat Oncol **14** (2004), no. 1, 65–75.
- [8] C. Plathow, C. Fink, S. Ley, M. Puderbach, M. Eichinger, I. Zuna, A. Schmhil, and H.-U. Kauczor, *Measurement of tumor diameter-dependent mobility of lung tumors by dynamic mri.*, Radiother Oncol **73** (2004), no. 3, 349–354.
- [9] A. Schweikard, G. Glosser, M. Boduluri, M.J. Murphy, and J.R. Adler, *Robotic motion compensation for respiratory movement during radiosurgery.*, Comput Aided Surg **5** (2000), no. 4, 263–277.
- [10] M.A. Staniszevska, *A modification of cristy's mathematical human phantoms for monte carlo simulation*, J Radiol Prot **12** (1992), 85–92.
- [11] T. Vik, S. Kabus, J. von Berg, K. Ens, S. Dries, T. Klinder, and C. Lorenz, *Validation and comparison of registration methods for free-breathing 4d lung ct*, vol. 6914, SPIE, 2008, p. 69142P.
- [12] P.-F. Villard, M. Beuve, B. Shariat, V. Baudet, and F. Jaillet, *Simulation of lung behaviour with finite elements: influence of bio-mechanical parameters*, Third International Conference on Medical Information Visualisation - Biomedical Visualisation, 2005. (MediVis 2005). Proceedings., 5-7 July 2005, pp. 9–14.
- [13] R. Werner, J. Ehrhardt, R. Schmidt, and H. Handels, *Modeling respiratory lung motion a biophysical approach using finite element methods*, Medical Imaging 2008: Physiology, Function, and Structure from Medical Images. Proc. SPIE (San Diego, USA), vol. Vol. 6916, Feb 2008, pp. 0N1–11.
- [14] T. Zhang, N.P. Orton, T.R. Mackie, and B.R. Paliwal, *Technical note: A novel boundary condition using contact elements for finite element based deformable image registration.*, Med Phys **31** (2004), no. 9, 2412–2415.

Acknowledgements

We would like to thank D. Low and W. Lu from the Washington University School of Medicine, St. Louis (USA), for providing the 4D CT data used in this study.